Chemical Physics 86 (1984) 147–159
North-Holland, Amsterdam

HIGH-RESOLUTION MOLECULAR-BEAM SPECTROSCOPY OF NaCN AND $Na^{13}CN$

J.J. VAN VAALS [1], W. Leo MEERTS and A. DYMANUS

Fysisch Laboratorium, Katholieke Universiteit, Toernooiveld, 6525 ED Nijmegen, The Netherlands

Received 21 November 1983

The sodium cyanide molecule was studied by molecular-beam electric-resonance spectroscopy in the microwave region. We used the seeded-beam technique to produce a supersonic beam with strong translational, rotational and vibrational cooling. In the frequency range 9.5–40 GHz we observed and identified for NaCN 186 and for $Na^{13}CN$ 107 hyperfine transitions in 20 and 16 rotational transitions, respectively, all in the ground vibrational state. The rotational, the five quartic and three sextic centrifugal distortion constants of NaCN are: $A''=57921.954(7)$ MHz, $B''=8369.312(2)$ MHz, $C''=7272.712(2)$ MHz. All quadrupole and several spin–rotation coupling constants for the hyperfine interaction were evaluated. The quadrupole coupling constants (in MHz) for NaCN are: $eQq_{aa}(\mathrm{Na})=-5.344(5)$, $eQq_{bb}=2.397(7)$, $eQq_{aa}(\mathrm{N})=2.148(4)$, $eQq_{bb}(\mathrm{N})=-4.142(5)$. From these constants and those of $Na^{13}CN$ we have determined the principal components of the quadrupole coupling tensor for potassium and nitrogen. The structure of sodium cyanide evaluated from the rotational constants of NaCN and $Na^{13}CN$ was found to be T shaped, similar to the structure of KCN but completely different from the linear isocyanide configuration of LiNC. The effective structural parameters for sodium cyanide in the ground vibrational state are: $r_{CN}=1.170(4)$ Å, $r_{NaC}=2.379(15)$ Å, $r_{NaN}=2.233(15)$ Å, in gratifying agreement with ab initio calculations. Both the geometrical structure and the hyperfine coupling justify the conclusion that the CN group in gaseous sodium cyanide approximately can be considered as a free CN^- ion.

1. Introduction

The molecular structure of alkali metal cyanides ☆ is difficult to predict. Since the first successful determination of the structure of gaseous potassium cyanide, which was found to be T shaped [1], several ab initio calculations of the potential-energy surface and equilibrium structure of KCN were performed [2–4]. Recently, two ab initio calculations of the structure of NaCN became available [3,4]. Both calculations predicted a T-shaped structure for sodium cyanide. However, as is illustrated by Marsden [4], the quality of the basis sets used in the SCF calculations and the inclusion of electron correlation influences the calculated potential-energy surface and the estimated equilibrium geometries drastically.

Ismail et al. [5] concluded from vibrational isotope effects of sodium cyanide in inert-gas matrices that the molecule has a linear cyanide configuration.

Earlier we reported preliminary results [6] for the first successful observation of the rotational spectrum of the most abundant isotopic species of sodium cyanide. The structure was found to be T shaped, and with the assumption of a fixed CN bond length an effective structure for the ground vibrational state was calculated.

In the current work we discuss a more elaborate study of the rotational and hyperfine spectra of NaCN and $Na^{13}CN$. We used the molecular-beam electric-resonance (MBER) spectrometer to observe for NaCN 186 and for $Na^{13}CN$ 107 hyperfine transitions in 20 and 16 rotational transitions, respectively. The hyperfine structure was analysed

[1] Present address: Philips Research Laboratories, 5600 MD Eindhoven, The Netherlands.

☆ In this paper the alkali metal cyanides are denoted by MCN (where M represents the alkali metal), whatever the structure may be, and the atomic symbol designates the most abundant isotope, unless specified otherwise.

and for each isotopic species we evaluated the quadrupole coupling constants and some spin–rotation constants. All rotational transitions, measured in the frequency range 9.5–40 GHz, originated in the ground vibrational state of the molecule and could be fitted to an asymmetric-rotor model. We determined the three rotational and eight distortion constants for NaCN and $Na^{13}CN$.

Since spectroscopic information from two isotopic species is now available, a more accurate structure can be calculated without assuming a CN bond length of 1.169 Å, as done before [6]. The result is in very good agreement with the preliminary structure [6].

The molecular parameters established experimentally are compared with the results of ab initio calculations [3,4]. The agreement is gratifying.

The principal components of the quadrupole coupling tensor for sodium and nitrogen were evaluated from the results for the two isotopic species. These values and the structure indicate that the CN group in sodium cyanide can be considered as an almost unperturbed CN^- ion.

2. Experimental results

The sodium cyanide molecule was studied by molecular-beam electric-resonance spectroscopy at microwave frequencies. This method furnishes high sensitivity at very high resolution, in the order of 10 kHz. The spectrometer has been described elsewhere [1,6–8].

The molecular beam was produced in a supersonic expansion of a mixture of sodium cyanide diluted in argon through a 130 μm nozzle at a backing pressure of 1 bar. The temperature of the supply chamber of the stainless-steel oven was held at 1100 K, which corresponds according to Ingold [9] and Porter [10] to a vapour pressure of monomeric sodium cyanide of 0.8–1.0 mbar. The nozzle chamber temperature was kept at 1300 K, to avoid clogging. Maintaining a stable molecular beam at the high temperatures necessary to obtain sufficient vapour pressure of monomeric NaCN, was handicapped by the instability of the cyanide molecule due to decomposition of the compound by wall reactions in the double chamber oven and thermal dissociation. The spectrum of $Na^{13}CN$ was obtained with a 90% isotopically enriched sample.

As a consequence of the seeded-beam technique, the internal temperatures of the sodium cyanide molecules were decreased strongly, concentrating the population in the low J states of the ground vibrational state. The intensity of the measured transitions was hereby enhanced and the rotational spectra were simplified drastically because no molecules in excited vibrational states were observed, facilitating analysis and identification considerably.

The rotational transitions of both isotopic species were identified by the observed hyperfine structure, the optimum voltages for the state selector field of the MBER spectrometer, and the optimum microwave radiation power irrigated to induce the transitions [1,11].

The hyperfine structure of the rotational transitions was analysed with a computer program including quadrupole, spin–rotation and spin–spin interaction based on the hyperfine hamiltonian and representation outlined in the paper on KCN [11]. The energy states obtained from diagonalization of the hamiltonian matrix are labeled by the quantum numbers J and F, and by a pseudo spin quantum number ε, where J is the molecular rotational angular momentum and F is the total angular momentum. For a given J and F, the state lowest in energy is denoted with $\varepsilon = 1$; the higher states are labeled by $\varepsilon = 2, 3, \ldots$ in order of increasing energy.

Starting values for the quadrupole coupling constants were obtained * from the ab initio field gradients calculated by Klein et al. [3], with a correction applied on these values corresponding to the difference between the ab initio [4] and the experimental [11] results for the quadrupole interaction in KCN. In a step by step calculation we succeeded in analysing the hyperfine structure of NaCN. All observed hyperfine transitions were identified. The quadrupole coupling constants eQq_{aa}-(Na), eQq_{bb}(Na), eQq_{aa}(N) and eQq_{bb}(N), and four spin–rotation coupling constants:

* We employed $Q(^{23}Na) = 0.116$ barn and $Q(^{14}N) = 0.0166$ barn. These values are from ref. [12].

Table 1
Hyperfine coupling constants for the ground vibrational state of NaCN and $Na^{13}CN$

Constant	NaCN	$Na^{13}CN$	Unit
eQq_{aa}(Na)	−5.344(5)	−5.328(12)	MHz
eQq_{bb}(Na)	2.398(7)	2.387(15)	MHz
eQq_{bb}(N)	2.148(4)	2.130(7)	MHz
eQq_{bb}(N)	−4.142(5)	−4.122(8)	MHz
M_{bb}(Na)	1.09(20)	–	kHz
M_{cc}(Na)	0.96(31)	–	kHz
M_{aa}(N)	13.7(3.5)	13.6(6.5)	kHz
M_{cc}(N)	1.88(42)	–	kHz
D_{aa}(Na–N)	−0.3714	−0.3674	kHz
D_{bb}(Na–N)	0.1651	0.1610	kHz

M_{bb}(Na), M_{cc}(Na), M_{aa}(N) and M_{cc}(N) were determined in a least-squares fit of the hyperfine splittings.

The hyperfine spectrum of $Na^{13}CN$ was analysed by a similar approach. For this molecule we started with the quadrupole coupling constants evaluated for NaCN. The contribution of the nuclear spin ($I = \frac{1}{2}$) of ^{13}C to the hyperfine structure has been neglected in the analysis because no additional splitting or broadening of the sodium–nitrogen hyperfine lines could be observed. From the analysis of the hyperfine spectrum all quadrupole coupling constants and the spin–rotation coupling constant M_{aa}(N) have been obtained.

For both molecules we fixed the remaining spin–rotation coupling constants at zero in the fit, since these could not be determined significantly. The spin–spin coupling constants D_{aa}(Na–N) and D_{bb}(Na–N) were constrained in the fit at the values calculated [11] from the geometry.

All observed hyperfine transitions (186 and 107 in 20 and 16 rotational transitions for NaCN and $Na^{13}CN$, respectively) are listed in the appendix. The results for the hyperfine coupling constants * for both isotopic species in the ground vibrational state are presented in table 1. The values of eQq_{cc} and D_{cc} can be obtained by using Laplace's equation. The variance ** for the least-squares fit of the hyperfine structure was $\sigma = 0.32$ for NaCN and $\sigma = 0.44$ for $Na^{13}CN$. The quadrupole coupling constants are discussed in section 4.

The hyperfine-free origins of the rotational transitions, established in the fit of the hyperfine spectra for NaCN and $Na^{13}CN$, are given in table 2. An impression of the observed rotational spectra in the frequency region 9.5–40 GHz of the two isotopic species in the ground vibrational state is presented in fig. 1. Both *a*-type and *b*-type transitions have been observed. The hyperfine-free rotational transition frequencies ν_0 were fitted for both molecules to an asymmetric-rotor model [11,13] without invoking the planarity conditions for the τ [11,14]. The quality of the fit of the rotational structure is good ($\sigma = 0.53$ for NaCN and $\sigma = 0.44$ for $Na^{13}CN$). We obtained for both isotopic species the rotational constants (A'', B'', and C''), the quartic centrifugal distortion constants (τ'_{aaaa}, τ'_{bbbb}, τ'_{cccc}, τ_1 and τ_2), and three sextic centrifugal distortion constants (H_{JK}, H_{KJ} and h_{JK}). The best-fit values are listed in table 3. The remaining four sextic distortion constants (H_J, H_K, h_J and h_K) could not well be determined in the fit and were fixed at zero. Table 3 also gives the τ-planarity defect [14] $\Delta\tau$.

Table 4 lists the τ-free rotational constants A, B and C, the centrifugal distortion constants τ_{aaaa}, τ_{bbbb}, τ_{aabb} and τ_{abab}, and the inertial defect [11] ΔI for NaCN and $Na^{13}CN$ in the ground vibrational state, derived by imposing the planarity condition [14], and the effective moments of inertia (I_a, I_b and I_c) evaluated *** from the τ-free rotational constants.

3. Structure

An exact evaluation of the structure requires rotational information of at least two isotopic

* All uncertainties stated in this paper represent three times the standard deviation as determined by the least-squares fit.

** The variance σ is defined as $[\chi^2/(n-m)]^{1/2}$ with χ^2 defined as usual in a least-squares fit, n the number of spectral lines and m the number of parameters in the fit.

*** We employed $h = 6.626176(36)\times10^{-34}$ J s. This value is from ref. [15].

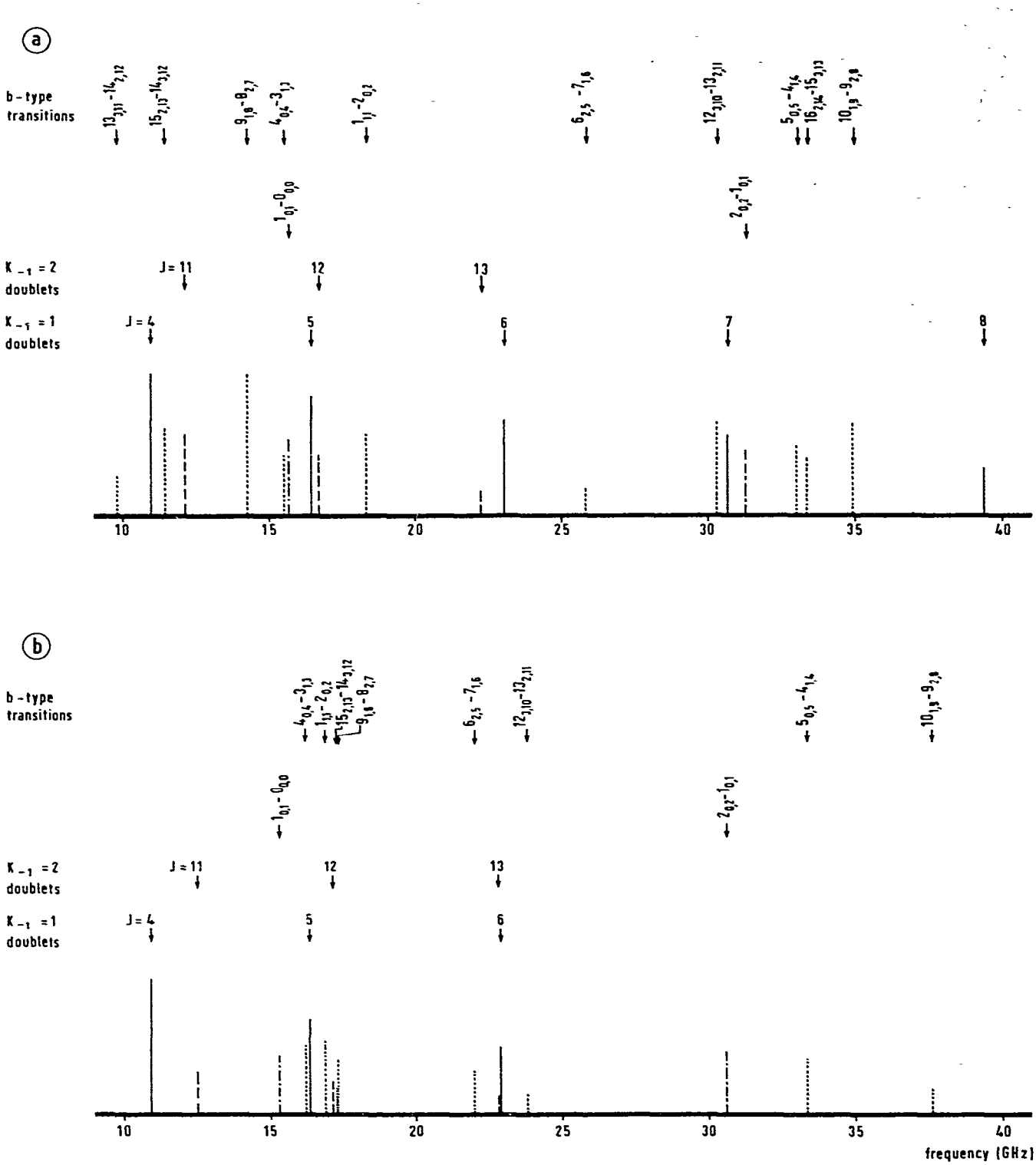

Fig. 1. Observed rotational transitions of NaCN (a) and $Na^{13}CN$ (b) in the ground vibrational state in the frequency region 9.5–40 GHz. The rotational transitions are indicated by $J'_{K_{-1},K_1} \rightarrow J''_{K_{-1},K_1}$. $K_{-1}=1$ doublets are transitions $J_{1,J-1} \rightarrow J_{1,J}$ and $K_{-1}=2$ doublets are transitions $J_{2,J-2} \rightarrow J_{2,J-1}$.

Table 2
Frequencies (in MHz) of the observed [a] and calculated hyperfine-free origins of the rotational transitions of NaCN and $Na^{13}CN$ in the ground vibrational state

Isotope	J'	K'_{-1}	K'_1	J''	K''_{-1}	K''_1	Type	Observed frequency	Obs.−calc.
NaCN	1	0	1	0	0	0	*a*	15640.3280(30)	0.0006
	2	0	2	1	0	1	*a*	31262.3341(30)	−0.0003
	4	1	3	4	1	4	*a*	10962.9463(20)	−0.0012
	5	1	4	5	1	5	*a*	16439.8314(30)	0.0020
	6	1	5	6	1	6	*a*	23005.2519(30)	0.0004
	7	1	6	7	1	7	*a*	30652.1941(40)	−0.0014
	8	1	7	8	1	8	*a*	39369.7637(50)	0.0007
	11	2	9	11	2	10	*a*	12153.1380(30)	−0.0001
	12	2	10	12	2	11	*a*	16691.9700(50)	0.0007
	13	2	11	13	2	12	*a*	22246.513(14)	−0.0028
	1	1	1	2	0	2	*b*	18289.3222(20)	−0.0002
	4	0	4	3	1	3	*b*	15497.1375(20)	−0.0009
	5	0	5	4	1	4	*b*	33010.2203(30)	0.0014
	6	2	5	7	1	6	*b*	25796.2003(50)	−0.0002
	9	1	8	8	2	7	*b*	14251.7157(40)	0.0008
	10	1	9	9	2	8	*b*	34919.1656(40)	−0.0008
	12	3	10	13	2	11	*b*	30238.988(22)	0.0206
	13	3	11	14	2	12	*b*	9783.5098(30)	−0.0007
	15	2	13	14	3	12	*b*	11402.6720(50)	−0.0011
	16	2	14	15	3	13	*b*	33303.6225(40)	0.0001
$Na^{13}CN$	1	0	1	0	0	0	*a*	15304.7785(70)	0.0019
	2	0	2	1	0	1	*a*	30590.6388(60)	−0.0025
	4	1	3	4	1	4	*a*	10908.6373(50)	−0.0021
	5	1	4	5	1	5	*a*	16358.0861(40)	0.0002
	6	1	5	6	1	6	*a*	22890.1355(70)	0.0013
	11	2	9	11	2	10	*a*	12507.2515(50)	−0.0006
	12	2	10	12	2	11	*a*	17156.985(10)	0.0043
	13	2	11	13	2	12	*a*	22834.293(19)	−0.0069
	1	1	1	2	0	2	*b*	16883.9590(60)	0.0014
	4	0	4	3	1	3	*b*	16209.3468(40)	−0.0002
	5	0	5	4	1	4	*b*	33365.0025(40)	0.0008
	6	2	5	7	1	6	*b*	22000.8898(50)	−0.0001
	9	1	8	8	2	7	*b*	17302.5009(50)	0.0005
	10	1	9	9	2	8	*b*	37585.577(10)	−0.0023
	12	3	10	13	2	11	*b*	23823.073(10)	0.0003
	15	2	13	14	3	12	*b*	17281.945(10)	0.0002

[a] The observed frequencies are evaluated in the least-squares fit of the observed hyperfine spectrum.

species, which is now available. The effective moments of inertia for NaCN and $Na^{13}CN$, listed in table 4, were used to calculate the structural parameters of sodium cyanide in the ground vibrational state. The resulting T-shaped structure presented in table 5 is in close agreement with the structure we reported earlier [6]. This shows that the assumption $r_{CN}(NaCN) \approx r_{CN}(KCN)$ used to obtain a preliminary structure in that communication [6] was correct.

The values of the calculated structural parameters are well within the uncertainties given in table 5, if the geometry of sodium cyanide is computed from any combination of four moments of inertia of the two isotopic species, with the limitation that I_a always has to be taken into account. This limitation can be explained from the same considerations as discussed for potassium cyanide [11].

Table 3
Rotational constants for the ground vibrational state of NaCN and $Na^{13}CN$

Constant	NaCN	$Na^{13}CN$	Unit
A''	57921.954(7)	55674.366(14)	MHz
B''	8369.312(2)	8198.767(3)	MHz
C''	7272.712(2)	7107.582(3)	MHz
τ'_{aaaa}	−4.026(10)	−4.084(16)	MHz
τ'_{bbbb}	−0.0833(2)	−0.0833(3)	MHz
τ'_{cccc}	−0.0459(2)	−0.0445(3)	MHz
τ_1	−3.3283(43)	−3.0809(65)	MHz
τ_2	−0.3670(6)	−0.3454(9)	MHz
H_{JK}	−15.6(6)	−14.2(1.2)	Hz
H_{KJ}	285 (13)	270 (22)	Hz
h_{JK}	−10.8(3.2)	−6.6(5.8)	Hz
$\Delta\tau$	−3.74(4)	−3.52(10)	kHz

4. Discussion

The large τ-planarity defect $\Delta\tau$ and inertial defect ΔI indicate that sodium cyanide is a floppy molecule, i.e. shows large amplitude motions in the bending direction. The bending vibrational frequency ω_2 evaluated [16] from the inertial defect is 179(35) cm^{-1} for NaCN and 176(35) cm^{-1} for $Na^{13}CN$. This is in good agreement with the frequency 168 cm^{-1}, obtained by Ismail et al. [5] for NaCN using the matrix-isolation technique. As with potassium cyanide, the value measured by Leroi and Klemperer [17] in an infrared absorption cell ($\omega_2 = 239(10)$ cm^{-1}) does not agree very well with the other results. An explanation as argued for KCN [5,11] may also be applicable here: the infrared absorption frequency should be assigned to another molecule, possibly NaOCN.

A summary of results of ab initio calculations for the structure and hyperfine quadrupole coupling constants is given in table 6. There is fair agreement between the ab initio and experimental structures. The quadrupole coupling constants were obtained [12] by transforming the field-gradient

Table 4
Derived molecular constants for the ground vibrational state of NaCN and $Na^{13}CN$

Constant	NaCN	$Na^{13}CN$	Unit
From τ_1 and τ_2, assuming planarity:			
A	57921.006	55673.470	MHz
B	8368.463	8197.977	MHz
C	7272.386	7107.294	MHz
τ_{aaaa}	−4.026	−4.084	MHz
τ_{bbbb}	−0.0833	−0.0833	MHz
τ_{aabb}	0.2664	0.2910	MHz
τ_{abab}	−1.8369	−1.7331	MHz
ΔI	0.3767	0.3827	amu Å^2
From τ_1 and τ'_{cccc}, assuming planarity:			
A	57921.075	55673.533	MHz
B	8368.473	8197.986	MHz
C	7272.342	7107.254	MHz
τ_{aaaa}	−4.026	−4.084	MHz
τ_{bbbb}	−0.0833	−0.0833	MHz
τ_{aabb}	0.1095	0.1474	MHz
τ_{abab}	−1.6979	−1.6062	MHz
ΔI	0.3772	0.3832	amu Å^2
From the τ-free rotational constants:			
I_a	8.72531(5)	9.07755(5)	amu Å^2
I_b	60.3909(25)	61.6468(25)	amu Å^2
I_c	69.4931(25)	71.1073(25)	amu Å^2

Table 5
The effective structural parameters for the ground vibrational state of sodium cyanide

Constant	Value (Å)
r_{CN}	1.170(4)
r_{NaC}	2.379(15)
r_{NaN}	2.233(15)

Table 6
Summary of results [a] of ab initio calculations on NaCN. The hyperfine coupling constants [12] are given for the ab initio structure, and in parentheses for the experimental structure (see text)

Constant	Klein et al. [3]	Marsden [4]	Unit
E(NaCN)	1640	1090	cm^{-1}
E(NaNC)	280	1340	cm^{-1}
r_{CN}	1.152	1.175	Å
r_{NaC}	2.470	2.376	Å
r_{NaN}	2.195	2.252	Å
eQq_{aa}(Na)	−5.491(−6.295)	–	MHz
eQq_{bb}(Na)	1.828(2.632)	–	MHz
eQq_{aa}(N)	1.674(2.001)	–	MHz
eQq_{bb}(N)	−3.517(−3.844)	–	MHz

[a] The quantities E(NaCN) and E(NaNC) are the energies relative to the T-shaped configuration of the linear cyanide and isocyanide configurations, respectively.

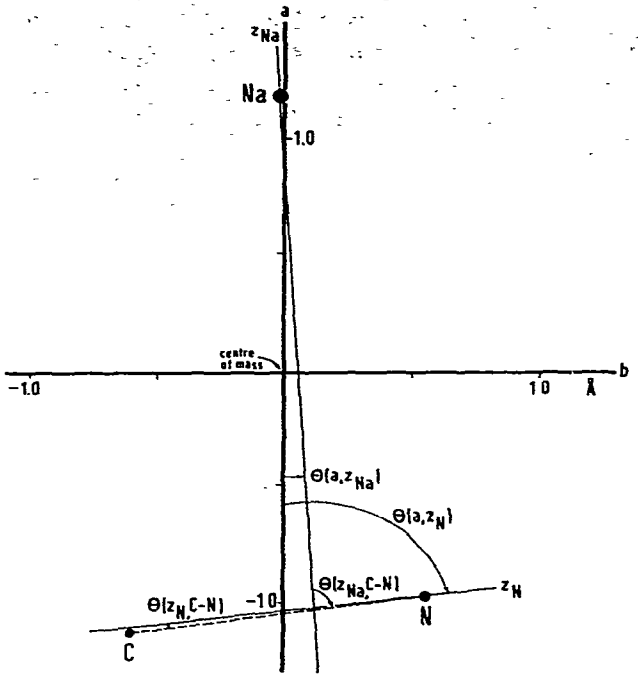

Fig. 2. Orientation of the principal axes of inertia (a, b, c) and the principal axes of the field gradient (x, y, z) in the sodium cyanide molecule. The c and y axes coincide and are perpendicular to the molecular plane. The subscripts Na and N are added to clearify the distinction between the sodium and the nitrogen quadrupole principal axes.

matrices calculated by Klein et al. [3] to the principal inertia axes system of the ab initio structure, and of the experimental structure, respectively. The results for the transformation to the principal axes system of the experimental structure are in better agreement with the accurate experimental values listed in table 1 than the results with respect to the ab initio structure.

The principal components of the quadrupole coupling tensors for sodium (eQq_x(Na) and eQq_z(Na)) and nitrogen (eQq_x(N) and eQq_z(N)) in sodium cyanide were determined by the method of Posener [18]. The results, including the asymmetry parameter for the quadrupole coupling $\eta = (eQq_x - eQq_y)/eQq_z$ and the angles $\theta(a, z)$ and $\theta(z$, C–N), defined in fig. 2, are presented in table 7. The axes of the principal inertial and principal quadrupole systems are denoted a, b, c and x, y, z, respectively. The principal axis z is chosen as the axis for which the coupling of the nucleus has nearly axial symmetry.

Table 7
Principal hyperfine quadrupole coupling constants for sodium cyanide in the ground vibrational state

Constant	Sodium	Nitrogen	Unit
eQq_x	2.429(10)	2.225(7)	MHz
eQq_z	−5.375(9)	−4.219(7)	MHz
η	0.096(4)	0.055(4)	
$\theta(a, z)$	−3.6(8)	83.7(3)	degree
$\theta(z$, C–N)	86.3(8)	−1.0(3)	degree

Since $\theta(z_N$, C–N) and η_N are small, the field gradient at the nitrogen nucleus is approximately symmetric about the bond axis between the carbon and the nitrogen nucleus. The experimental values of r_{CN} and eQq_z(N) are in close agreement with the results of ab initio calculations for the free CN^- ion: the equilibrium value of $r_{CN} = 1.173(2)$ Å [19] and $eQq(N) = -4.090$ MHz ☆. From these arguments we conclude that in sodium cyanide, like in KCN [11], the CN group can be considered as an almost unperturbed CN^- ion.

The large anharmonicity and the low barriers of the potential-energy surface in the bending direction [3,4] are most likely the origin of the disagreement among the available thermodynamic data [5,10,21] for sodium cyanide. To remove those discrepancies it will be imperative to take the exact potential-energy surface into account.

Table 6 shows that the differences between the ab initio calculated values of E(NaCN) and E(NaNC) are very large. This implies that the reliability of the computed potentials is rather questionable. With the accurate experimental determination of the T-shaped structure of NaCN in the ground vibrational state, the bottom of the intermolecular potential is now well located. Recently we have started experiments in which the excited vibrational states of the alkali metal cyanides are investigated. These studies will hopefully provide a more accurate picture of the potential-energy surface and a better understanding of the weak internal interactions in floppy molecules.

☆ This result was evaluated [12] from the field gradient computed by Wormer [20] in a SCF calculation using 54 contracted gaussian-type orbitals at $r_{CN} = 1.174$ Å.

Acknowledgement

The authors wish to express their gratitude to Dr. P.E.S. Wormer for calculating the field gradient at the nitrogen nucleus in the CN^- ion, and to Dr. C.J. Marsden for communicating his result on the ab initio structure of NaCN. They thank Dr. J.P. Bekooy for the many fruitful discussions they have enjoyed with him. This work is part of the research program of the Stichting voor Fundamenteel Onderzoek der Materie (FOM) and has been made possible by financial support from the Nederlandse Organisatie voor Zuiver-Wetenschappelijk Onderzoek (ZWO).

Appendix

Frequencies (in MHz) of the observed and calculated hyperfine transitions of NaCN in the ground vibrational state.

$F_\varepsilon' \to F_\varepsilon''$	Obs.frequency	Obs.-calc.
Rotational transition $1_{0,1} \to 0_{0,0}$:		
$7/2_1 \to 5/2_1$	15640.4907(70)	0.0003
$5/2_2 \to 5/2_1$	15640.9925(40)	0.0000
$1/2_2 \to 1/2_1$	15641.6909(50)	0.0002
$3/2_3 \to 3/2_1$	15641.8645(40)	-0.0003
Rotational transition $2_{0,2} \to 1_{0,1}$:		
$5/2_3 \to 3/2_2$	31262.7269(70)	-0.0015
$7/2_2 \to 7/2_1$	31263.0095(70)	-0.0006
$5/2_3 \to 5/2_1$	31263.7463(60)	0.0005
$3/2_3 \to 3/2_2$	31263.7463(60)	-0.0005
$1/2_2 \to 1/2_1$	31264.5149(80)	0.0013
$3/2_3 \to 5/2_1$	31264.7650(60)	0.0009
Rotational transition $4_{1,3} \to 4_{1,4}$:		
$7/2_1 \to 9/2_1$	10962.4800(80)	-0.0008
$11/2_1 \to 9/2_1$	10962.9114(50)	-0.0035
$3/2_1 \to 5/2_1$	10963.0483(60)	-0.0048
$7/2_3 \to 7/2_3$	10963.0483(60)	-0.0035
$9/2_1 \to 9/2_1$	10963.1907(60)	0.0012
$9/2_2 \to 9/2_1$	10963.4168(70)	0.0010
$7/2_2 \to 7/2_2$	10963.5017(80)	-0.0004
$13/2_1 \to 11/2_1$	10963.5843(60)	0.0007
$9/2_3 \to 7/2_2$	10964.0700(80)	0.0016
$7/2_2 \to 9/2_1$	10964.1214(80)	0.0029
$9/2_3 \to 11/2_1$	10964.3212(80)	0.0055
$7/2_3 \to 9/2_1$	10965.0533(50)	0.0015
$11/2_2 \to 11/2_1$	10965.1937(70)	0.0020
$5/2_2 \to 7/2_2$	10965.2681(80)	0.0040
$11/2_2 \to 9/2_1$	10965.562(15)	0.0016
$5/2_2 \to 7/2_1$	10965.588(20)	-0.0068

$F_\varepsilon' \to F_\varepsilon''$	Obs.frequency	Obs.-calc.
Rotational transition $5_{1,4} \to 5_{1,5}$:		
$11/2_2 \to 13/2_1$	16440.034(10)	-0.0021
$5/2_1 \to 7/2_1$	16440.034(10)	-0.0094
$9/2_3 \to 7/2_2$	16440.2233(80)	0.0041
$11/2_3 \to 13/2_2$	16440.274(10)	0.0048
$9/2_2 \to 11/2_2$	16440.274(10)	-0.0027
$11/2_2 \to 11/2_1$	16440.4187(70)	0.0000
$9/2_2 \to 9/2_1$	16440.7467(80)	-0.0001
$11/2_3 \to 9/2_2$	16441.0094(70)	0.0034
$9/2_3 \to 11/2_2$	16441.1173(90)	0.0008
$9/2_3 \to 9/2_2$	16441.3295(90)	0.0026
$11/2_3 \to 11/2_1$	16441.546(10)	0.0016
$9/2_3 \to 9/2_1$	16441.583(10)	-0.0038
$9/2_3 \to 11/2_1$	16441.863(10)	-0.0017
$13/2_2 \to 13/2_1$	16442.1532(70)	-0.0012
$13/2_2 \to 11/2_1$	16442.5376(90)	0.0008
$7/2_2 \to 9/2_1$	16442.5376(90)	-0.0019
Rotational transition $6_{1,5} \to 6_{1,6}$:		
$15/2_1 \to 15/2_2$	23003.8375(70)	0.0024
$13/2_1 \to 15/2_1$	23004.9912(60)	0.0009
$13/2_1 \to 13/2_1$	23005.3872(80)	-0.0013
$13/2_2 \to 11/2_2$	23005.4328(80)	0.0018
$13/2_2 \to 13/2_1$	23005.9321(60)	-0.0006
$11/2_2 \to 11/2_1$	23006.1968(70)	0.0022
$13/2_3 \to 15/2_1$	23006.5478(90)	0.0027
$11/2_3 \to 11/2_2$	23006.7162(90)	-0.0047
$11/2_3 \to 13/2_1$	23007.2224(60)	-0.0002
$15/2_2 \to 15/2_1$	23007.6132(70)	0.0025
$15/2_2 \to 13/2_1$	23008.0056(50)	-0.0032

$F_\varepsilon'\to F_\varepsilon''$	Obs. frequency	Obs.-calc.
Rotational transition $7_{1,6}\to7_{1,7}$:		
$15/2_2\to15/2_1$	30652.9544(80)	0.0042
$15/2_3\to15/2_2$	30653.174(10)	-0.0033
$11/2_2\to13/2_3$	30653.174(10)	-0.0032
$15/2_3\to13/2_1$	30653.6290(90)	0.0000
$13/2_3\to15/2_1$	30654.115(10)	0.0017
$17/2_2\to15/2_1$	30654.981(10)	-0.0017
Rotational transition $8_{1,7}\to8_{1,8}$:		
$15/2_1\to17/2_3$	39367.5894(80)	0.0027
$19/2_1\to21/2_1$	39367.841(10)	-0.0017
$17/2_3\to17/2_3$	39369.589(12)	0.0019
$17/2_1\to15/2_1$	39369.626(12)	-0.0034
$19/2_2\to17/2_1$	39372.569(12)	-0.0021
Rotational transition $11_{2,9}\to11_{2,10}$:		
$23/2_2\to23/2_3$	12152.770(12)	0.0027
$21/2_2\to21/2_3$	12152.797(10)	0.0028
$19/2_1\to19/2_1$	12152.8815(80)	0.0032
$21/2_1\to21/2_1$	12152.8815(80)	0.0007
$23/2_1\to23/2_1$	12152.9328(80)	-0.0008
$21/2_3\to21/2_3$	12153.085(10)	0.0000
$23/2_3\to23/2_3$	12153.126(10)	-0.0023
$23/2_2\to23/2_2$	12153.3684(70)	0.0000
$21/2_2\to21/2_2$	12153.4574(80)	-0.0013
$19/2_2\to19/2_2$	12153.608(12)	0.0000
$25/2_2\to25/2_2$	12153.608(12)	-0.0063
$23/2_3\to23/2_2$	12153.737(20)	0.0078
$21/2_3\to21/2_2$	12153.737(20)	-0.0115
Rotational transition $12_{2,10}\to12_{2,11}$:		
$21/2_1\to21/2_1$	16691.681(12)	0.0040
$23/2_1\to23/2_1$	16691.681(12)	0.0011
$25/2_1\to25/2_1$	16691.733(10)	-0.0007
$21/2_2\to21/2_2$	16692.510(15)	0.0023
$27/2_2\to27/2_2$	16692.510(15)	-0.0043
$25/2_3\to25/2_2$	16692.618(20)	0.0008
$23/2_3\to23/2_2$	16692.618(20)	-0.0084

$F_\varepsilon'\to F_\varepsilon''$	Obs. frequency	Obs.-calc.
Rotational transition $13_{2,11}\to13_{2,12}$:		
$23/2_1\to23/2_1$	22246.190(20)	0.0017
$25/2_1\to25/2_1$	22246.190(20)	-0.0017
Rotational transition $1_{1,1}\to2_{0,2}$:		
$3/2_1\to1/2_2$	18286.4453(60)	0.0010
$3/2_1\to3/2_3$	18286.5604(60)	-0.0006
$1/2_1\to1/2_2$	18286.8512(60)	-0.0015
$1/2_1\to3/2_3$	18286.9688(60)	-0.0006
$5/2_1\to7/2_2$	18287.4524(40)	0.0002
$3/2_1\to5/2_3$	18287.5793(80)	-0.0001
$1/2_2\to3/2_3$	18287.939(10)	0.0010
$3/2_2\to1/2_2$	18288.035(12)	0.0009
$3/2_2\to3/2_3$	18288.1499(60)	-0.0006
$5/2_2\to3/2_3$	18288.4936(80)	0.0020
$7/2_1\to7/2_2$	18288.5798(80)	0.0004
$5/2_2\to7/2_2$	18289.046(12)	-0.0003
$7/2_1\to9/2_1$	18289.177(10)	-0.0022
$1/2_2\to3/2_2$	18289.2392(80)	0.0000
$5/2_2\to5/2_3$	18289.5111(60)	0.0012
$3/2_2\to5/2_2$	18289.699(10)	-0.0010
Rotational transition $4_{0,4}\to3_{1,3}$:		
$9/2_1\to7/2_2$	15496.588(10)	0.0016
$11/2_1\to9/2_1$	15496.799(10)	0.0014
$9/2_2\to7/2_2$	15496.8812(90)	-0.0019
$13/2_1\to11/2_1$	15496.976(10)	-0.0004
$7/2_2\to5/2_2$	15497.3310(60)	0.0017
$9/2_2\to9/2_1$	15497.4113(80)	-0.0003
$9/2_1\to7/2_1$	15497.4686(80)	0.0020
$9/2_2\to7/2_1$	15497.7611(90)	-0.0020
$7/2_2\to5/2_1$	15497.8324(60)	0.0009
$11/2_2\to9/2_2$	15498.0074(60)	-0.0015
$7/2_2\to7/2_1$	15498.0987(80)	-0.0014
$7/2_3\to7/2_2$	15498.1309(80)	-0.0003
$9/2_3\to7/2_1$	15498.4144(70)	0.0014
$5/2_2\to3/2_1$	15498.6488(70)	0.0015

$F_\varepsilon' \to F_\varepsilon''$	Obs.frequency	Obs.-calc.
$5/2_2 \to 5/2_2$	15498.7263(60)	-0.0018
$5/2_2 \to 5/2_1$	15499.2294(80)	-0.0010
Rotational transition $5_{0,5} \to 4_{1,4}$:		
$7/2_1 \to 7/2_2$	33009.9400(80)	-0.0040
$9/2_3 \to 7/2_3$	33010.0532(80)	0.0052
$11/2_2 \to 9/2_2$	33010.0532(80)	0.0008
$11/2_2 \to 11/2_1$	33010.4874(70)	-0.0007
$9/2_2 \to 7/2_2$	33010.5478(80)	-0.0014
$7/2_2 \to 7/2_3$	33010.5478(80)	0.0054
$11/2_1 \to 9/2_1$	33010.5977(70)	-0.0012
$9/2_2 \to 9/2_1$	33011.1633(80)	-0.0023
$9/2_3 \to 9/2_2$	33011.2464(90)	0.0032
$11/2_3 \to 9/2_1$	33011.5669(80)	-0.0012
$7/2_2 \to 5/2_1$	33011.717(12)	0.0006
$9/2_3 \to 7/2_1$	33011.760(12)	-0.0022
$13/2_2 \to 11/2_1$	33011.8269(80)	0.0006
$7/2_2 \to 7/2_2$	33011.924(10)	-0.0025
$7/2_2 \to 7/2_1$	33012.2559(80)	-0.0009
Rotational transition $6_{2,5} \to 7_{1,6}$:		
$17/2_1 \to 17/2_2$	25794.752(20)	0.0038
$13/2_1 \to 13/2_3$	25794.845(25)	-0.0112
$15/2_1 \to 15/2_3$	25794.900(25)	-0.0084
$13/2_1 \to 15/2_3$	25795.103(10)	0.0013
$9/2_2 \to 11/2_2$	25795.223(15)	-0.0005
$11/2_2 \to 13/2_3$	25795.328(10)	0.0013
$13/2_3 \to 13/2_3$	25795.552(15)	0.0006
$9/2_1 \to 9/2_1$	25795.637(25)	-0.0122
$13/2_3 \to 13/2_2$	25796.268(25)	0.0092
Rotational transition $9_{1,8} \to 8_{2,7}$:		
$23/2_1 \to 21/2_1$	14251.4295(90)	0.0000
$19/2_2 \to 17/2_2$	14251.7595(70)	0.0035
$17/2_3 \to 15/2_3$	14251.9318(60)	-0.0035
$19/2_3 \to 17/2_3$	14252.0135(70)	0.0013
Rotational transition $10_{1,9} \to 9_{2,8}$:		
$17/2_1 \to 15/2_1$	34918.704(15)	0.0049
$19/2_1 \to 17/2_1$	34918.704(15)	0.0002
$19/2_2 \to 17/2_3$	34918.782(15)	0.0010
$21/2_1 \to 19/2_1$	34918.782(15)	-0.0028
$25/2_1 \to 23/2_1$	34918.8694(80)	-0.0019
$21/2_2 \to 19/2_2$	34919.254(10)	-0.0010
$19/2_2 \to 17/2_2$	34919.3997(80)	0.0007
$17/2_2 \to 15/2_2$	34919.954(15)	0.0042
$19/2_3 \to 17/2_2$	34919.954(15)	-0.0012
Rotational transition $12_{3,10} \to 13_{2,11}$:		
$21/2_2 \to 23/2_2$	30238.434(50)	0.0070
$27/2_2 \to 29/2_2$	30238.434(50)	0.0101
$25/2_3 \to 27/2_2$	30239.272(50)	0.0013
$25/2_1 \to 27/2_1$	30239.272(50)	-0.0094
$27/2_1 \to 29/2_1$	30239.272(50)	-0.0090
Rotational transition $13_{3,11} \to 14_{2,12}$:		
$29/2_2 \to 31/2_2$	9782.927(12)	0.0015
$23/2_2 \to 25/2_2$	9782.927(12)	-0.0039
$27/2_2 \to 29/2_3$	9782.956(10)	-0.0008
$25/2_2 \to 27/2_3$	9782.956(10)	-0.0015
$27/2_3 \to 29/2_3$	9783.3040(90)	0.0022
$25/2_3 \to 27/2_3$	9783.3680(80)	0.0005
$25/2_2 \to 27/2_2$	9783.3680(80)	-0.0016
$27/2_2 \to 29/2_2$	9783.463(12)	0.0000
$31/2_1 \to 33/2_1$	9783.723(12)	0.0034
$25/2_3 \to 27/2_2$	9783.777(15)	-0.0026
$27/2_1 \to 29/2_1$	9783.8080(90)	0.0009
$25/2_1 \to 27/2_1$	9783.841(12)	0.0008
$23/2_1 \to 25/2_1$	9783.841(12)	0.0001
Rotational transition $15_{2,13} \to 14_{3,12}$:		
$25/2_1 \to 23/2_1$	11402.391(12)	-0.0074
$35/2_1 \to 33/2_1$	11402.442(14)	0.0029
$31/2_2 \to 29/2_2$	11402.711(14)	0.0063
$29/2_2 \to 27/2_2$	11402.792(14)	-0.0021
$29/2_3 \to 27/2_3$	11402.847(14)	0.0025
$31/2_3 \to 29/2_3$	11402.916(14)	0.0060

$F_\varepsilon'\to F_\varepsilon''$	Obs. frequency	Obs.-calc.
$27/2_2\to25/2_2$	11403.268(15)	0.0003
$33/2_2\to31/2_2$	11403.268(15)	-0.0066
Rotational transition $16_{2,14}\to15_{3,13}$:		
$33/2_1\to31/2_1$	33303.310(12)	-0.0065
$35/2_1\to33/2_1$	33303.328(14)	0.0069
$27/2_1\to25/2_1$	33303.328(14)	-0.0025
$29/2_2\to27/2_2$	33304.2361(60)	0.0044
$35/2_2\to33/2_2$	33304.2361(60)	-0.0036

Frequencies (in MHz) of the observed and calculated hyperfine transitions of $Na^{13}CN$ in the ground vibrational state.

$F_\varepsilon'\to F_\varepsilon''$	Obs. frequency	Obs.-calc.
Rotational transition $1_{0,1}\to0_{0,0}$:		
$7/2_1\to5/2_1$	15304.941(10)	0.0029
$5/2_2\to3/2_1$	15305.4394(90)	0.0014
$1/2_2\to3/2_1$	15306.137(10)	-0.0017
$3/2_3\to1/2_1$	15306.3091(90)	-0.0024
Rotational transition $2_{0,2}\to1_{0,1}$:		
$5/2_1\to5/2_2$	30589.042(12)	0.0012
$5/2_3\to3/2_2$	30591.0338(90)	0.0038
$1/2_1\to1/2_1$	30591.122(10)	-0.0092
$1/2_2\to1/2_1$	30592.8166(90)	0.0007
$3/2_3\to5/2_1$	30593.0662(80)	0.0018
Rotational transition $4_{1,3}\to4_{1,4}$:		
$7/2_1\to7/2_2$	10907.563(10)	0.0073
$5/2_1\to7/2_2$	10907.9660(90)	-0.0038
$9/2_1\to9/2_2$	10908.073(12)	-0.0078
$7/2_1\to9/2_1$	10908.1789(90)	-0.0006
$9/2_1\to9/2_1$	10908.8840(80)	0.0001
$9/2_2\to9/2_1$	10909.1062(90)	-0.0005
$7/2_2\to7/2_2$	10909.188(10)	-0.0007
$13/2_1\to11/2_1$	10909.2701(70)	-0.0009
$9/2_3\to9/2_1$	10910.3717(80)	0.0030
$7/2_3\to7/2_1$	10910.4526(80)	0.0006
$11/2_2\to11/2_1$	10910.8728(80)	0.0007
Rotational transition $5_{1,4}\to5_{1,5}$:		
$13/2_1\to13/2_2$	16356.7424(80)	-0.0034
$9/2_1\to9/2_1$	16357.3796(80)	0.0045
$7/2_1\to9/2_2$	16357.4559(80)	-0.0008
$13/2_1\to11/2_1$	16358.0093(70)	-0.0020
$11/2_2\to9/2_2$	16358.1327(90)	0.0083
$11/2_1\to11/2_1$	16358.2787(80)	0.0018
$11/2_2\to11/2_1$	16358.6742(60)	0.0016
$9/2_2\to9/2_2$	16358.7384(90)	0.0017
$15/2_1\to13/2_1$	16358.7384(90)	-0.0016
$9/2_2\to9/2_1$	16358.9986(70)	-0.0044
$11/2_3\to9/2_1$	16359.5128(70)	0.0031
$9/2_3\to9/2_2$	16359.5717(90)	0.0012
$9/2_3\to11/2_1$	16360.1130(80)	-0.0057
$7/2_2\to7/2_1$	16360.282(10)	-0.0013
$13/2_2\to13/2_1$	16360.3962(70)	-0.0016
$13/2_2\to11/2_1$	16360.782(14)	0.0078
$7/2_2\to9/2_1$	16360.782(14)	-0.0067
Rotational transition $6_{1,5}\to6_{1,6}$:		
$11/2_1\to13/2_1$	22889.7345(80)	-0.0036
$11/2_3\to13/2_1$	22892.1012(70)	-0.0052

$F_\varepsilon' \to F_\varepsilon''$	Obs. frequency	Obs.-calc.
$15/2_2 \to 15/2_1$	22892.4825(90)	0.0001
$9/2_2 \to 11/2_1$	22892.8795(90)	0.0077
$15/2_2 \to 13/2_1$	22892.8795(90)	0.0054
Rotational transition $11_{2,9} \to 11_{2,10}$:		
$19/2_1 \to 19/2_1$	12506.9890(90)	0.0076
$21/2_1 \to 21/2_1$	12506.9890(90)	0.0053
$23/2_1 \to 23/2_1$	12507.0403(70)	-0.0049
$21/2_3 \to 21/2_3$	12507.1975(80)	-0.0069
$23/2_3 \to 23/2_3$	12507.2450(80)	-0.0017
$23/2_2 \to 23/2_2$	12507.4828(80)	0.0049
Rotational transition $12_{2,10} \to 12_{2,11}$:		
$21/2_1 \to 21/2_1$	17156.683(12)	0.0025
$23/2_1 \to 23/2_1$	17156.683(12)	-0.0002
$25/2_2 \to 25/2_2$	17157.219(12)	-0.0023
Rotational transition $13_{2,11} \to 13_{2,12}$:		
$23/2_1 \to 23/2_1$	22833.954(20)	-0.0018
$29/2_1 \to 29/2_1$	22834.034(20)	0.0018
Rotational transition $1_{1,1} \to 2_{0,2}$:		
$3/2_1 \to 1/2_2$	16881.092(10)	0.0025
$3/2_1 \to 3/2_3$	16881.209(10)	0.0027
$1/2_1 \to 1/2_2$	16881.499(12)	0.0029
$1/2_1 \to 3/2_3$	16881.612(12)	-0.0013
$5/2_1 \to 7/2_2$	16882.0966(80)	-0.0056
$3/2_1 \to 5/2_3$	16882.222(10)	-0.0039
$3/2_2 \to 3/2_3$	16882.788(14)	0.0009
$3/2_1 \to 1/2_1$	16882.788(14)	0.0132
$7/2_1 \to 9/2_1$	16883.817(14)	-0.0016
Rotational transition $4_{0,4} \to 3_{1,3}$:		
$11/2_1 \to 9/2_1$	16209.011(12)	0.0021
$9/2_3 \to 7/2_3$	16209.011(12)	-0.0007
$9/2_2 \to 7/2_2$	16209.090(10)	-0.0038
$13/2_1 \to 11/2_1$	16209.187(10)	0.0020
$7/2_2 \to 5/2_2$	16209.532(10)	0.0006
$9/2_1 \to 7/2_1$	16209.677(10)	0.0016
$9/2_2 \to 7/2_1$	16209.972(10)	0.0000

$F_\varepsilon' \to F_\varepsilon''$	Obs. frequency	Obs.-calc
$7/2_2 \to 5/2_1$	16210.0361(80)	-0.0010
$11/2_2 \to 9/2_2$	16210.2112(60)	0.0013
$9/2_3 \to 7/2_1$	16210.625(10)	0.0061
$5/2_2 \to 3/2_1$	16210.847(10)	-0.0028
$5/2_2 \to 5/2_1$	16211.426(12)	-0.0097
Rotational transition $5_{0,5} \to 4_{1,4}$:		
$11/2_2 \to 11/2_1$	33365.2705(80)	-0.0015
$9/2_2 \to 7/2_2$	33365.3241(80)	0.0026
$7/2_2 \to 7/2_1$	33365.3241(80)	-0.0002
$11/2_1 \to 9/2_1$	33365.3807(80)	-0.0008
$13/2_2 \to 11/2_2$	33365.7676(70)	0.0022
$9/2_2 \to 9/2_1$	33365.9441(80)	-0.0013
$9/2_3 \to 9/2_2$	33366.0299(80)	0.0000
$11/2_3 \to 9/2_1$	33366.353(10)	0.0040
$7/2_2 \to 7/2_1$	33367.028(10)	-0.0066
Rotational transition $6_{2,5} \to 7_{1,6}$:		
$13/2_2 \to 13/2_3$	21999.814(10)	0.0049
$15/2_2 \to 17/2_2$	21999.930(10)	-0.0033
$11/2_2 \to 13/2_3$	22000.018(12)	-0.0003
$13/2_2 \to 15/2_3$	22000.060(12)	-0.0023
$13/2_3 \to 15/2_3$	22000.491(10)	-0.0004
$11/2_3 \to 13/2_3$	22000.552(10)	-0.0023
$11/2_2 \to 13/2_2$	22000.7233(90)	0.0055
$13/2_2 \to 15/2_2$	22000.9714(80)	-0.0025
Rotational transition $9_{1,8} \to 8_{2,7}$:		
$15/2_1 \to 13/2_1$	17301.9974(80)	-0.0013
$17/2_1 \to 15/2_1$	17301.9974(80)	-0.0002
$19/2_2 \to 17/2_3$	17302.036(10)	0.0057
$23/2_1 \to 21/2_1$	17302.2148(80)	-0.0023
$19/2_2 \to 17/2_2$	17302.543(10)	0.0021
$17/2_3 \to 15/2_3$	17302.713(10)	-0.0019
Rotational transition $10_{1,9} \to 9_{2,8}$:		
$25/2_1 \to 23/2_1$	37585.280(12)	-0.0054
$17/2_2 \to 15/2_2$	37586.363(12)	0.0064
$23/2_2 \to 21/2_2$	37586.363(12)	-0.0010

$F_\varepsilon' \rightarrow F_\varepsilon''$	Obs.frequency	Obs.-calc.
Rotational transition $12_{3,10} \rightarrow 13_{2,11}$:		
$21/2_2 \rightarrow 23/2_2$	23822.504(14)	0.0021
$27/2_2 \rightarrow 29/2_2$	23822.504(14)	0.0001
$25/2_1 \rightarrow 27/2_1$	23823.365(14)	-0.0004
$27/2_1 \rightarrow 29/2_1$	23823.365(14)	-0.0017

$F_\varepsilon' \rightarrow F_\varepsilon''$	Obs.frequency	Obs.-calc.
Rotational transition $15_{2,13} \rightarrow 14_{3,12}$:		
$25/2_1 \rightarrow 23/2_1$	17281.667(14)	0.0012
$27/2_2 \rightarrow 25/2_2$	17282.549(12)	0.0005
$33/2_2 \rightarrow 31/2_2$	17282.549(12)	-0.0013

References

[1] T. Törring, J.P. Bekooy, W.L. Meerts, J. Hoeft, E. Tiemann and A. Dymanus, J. Chem. Phys. 73 (1980) 4875.
[2] P.E.S. Wormer and J. Tennyson, J. Chem. Phys. 75 (1981) 1245.
[3] M.L. Klein, J.D. Goddard and D.G. Bounds, J. Chem. Phys. 75 (1981) 3909.
[4] C.J. Marsden, J. Chem. Phys. 76 (1982) 6451; private communication.
[5] Z.K. Ismail, R.H. Hauge and J.L. Margrave, J. Mol. Spectry. 45 (1973) 304.
[6] J.J. van Vaals, W.L. Meerts and A. Dymanus, J. Chem. Phys. 77 (1982) 5245.
[7] J.J. van Vaals, W.L. Meerts and A. Dymanus, Chem. Phys. 82 (1983) 385.
[8] J.J. van Vaals, Ph.D. Thesis, Katholieke Universiteit Nijmegen, The Netherlands (1983).
[9] C.K. Ingold, J. Chem. Soc. 123 (1923) 885.
[10] R.F. Porter, J. Chem. Phys. 35 (1961) 318.
[11] J.J. van Vaals, W.L. Meerts and A. Dymanus, J. Mol. Spectry., submitted for publication.
[12] C.M. Lederer and V.S. Shirley, eds., Table of isotopes, 7th Ed. (Wiley, New York, 1978).
[13] J.K.G. Watson, J. Chem. Phys. 46 (1967) 1935; 48 (1968) 4517.
[14] W.H. Kirchhoff, J. Mol. Spectry, 41 (1972) 333.
[15] E.R. Cohen and B.N. Taylor, J. Phys. Chem. Ref. Data 2 (1973) 663.
[16] W. Gordy and R.L. Cook, Microwave molecular spectra (Interscience, New York, 1970).
[17] G.E. Leroi and W. Klemperer, J. Chem. Phys. 35 (1961) 774.
[18] D.W. Posener, Australian J. Phys. 13 (1960) 168.
[19] P.R. Taylor, G.B. Bacskay, N.S. Hush and A.C. Hurley, J. Chem. Phys. 70 (1979) 4481.
[20] P.E.S. Wormer, private communication.
[21] E.W. Guernsey and M.S. Sherman, J. Am. Chem. Soc. 48 (1926) 695;
JANAF thermochemical tables, 2nd Ed. (US Department of Commerce, National Bureau of Standards, Washington, 1971);
J.N. Mulvihill and L.F. Phillips, Chem. Phys. Letters 33 (1975) 608;
B.V. L'vov and L.A. Pelieva, Progr. Analyt. At. Spectry. 3 (1980) 65;
K. Skudlarski and M. Miller, Advan. Mass Spectrom. 8A (1980) 433; High Temp. Sci. 15 (1982) 151.